Temporal variability and driving factors of the carbonate system in the Aransas Ship Channel, TX, USA: A time-series study

Melissa R. McCutcheon[1], Hongming Yao[1,#], Cory J. Staryk[1], Xinping Hu[1]

[1] Harte Research Institute for Gulf of Mexico Studies, Texas A&M University – Corpus Christi, TX 78412, USA
[#] current address: Shenzhen Engineering Laboratory of Ocean Environmental Big Data Analysis and Application, Shenzhen Institute of Advanced Technology, Chinese Academy of Sciences, Shenzhen 518055, China

_____

Correspondence to: Melissa R. McCutcheon (melissa.mccutcheon@tamucc.edu)

Keywords: pCO_2, acidification, diel variability, seasonal variability, autonomous sensors

Abstract

The coastal ocean is affected by an array of co-occurring biogeochemical and anthropogenic processes, resulting in substantial heterogeneity in water chemistry, including carbonate chemistry parameters such as pH and partial pressure of CO_2 (pCO_2). To better understand coastal and estuarine acidification and air-sea CO_2 fluxes, it is important to study baseline variability and driving factors of carbonate chemistry. Using both discrete bottle sample collection (2014-2020) and hourly sensor measurements (2016-2017), we explored temporal variability, from diel to interannual scales, in the carbonate system (specifically pH and pCO_2) at the Aransas Ship Channel located in northwestern Gulf of Mexico. Using other co-located environmental sensors, we also explored the driving factors of that variability. Both sampling methods demonstrated significant seasonal variability at the location, with highest pH (lowest pCO_2) in the winter and lowest pH (highest pCO_2) in the summer. Significant diel variability was also evident from sensor data, but the time of day with elevated pCO_2/depressed pH was not consistent across the entire monitoring period, sometimes reversing from what would be expected from a biological signal. Though seasonal and diel fluctuations were smaller than many other areas previously studied, carbonate chemistry parameters were among the most important environmental parameters to distinguish between time of day and between seasons. It is evident that temperature, biological activity, freshwater inflow, and tide level (despite the small tidal range) are all important controls on the system, with different controls dominating at different time scales. The results suggest that the controlling factors of the carbonate system may not be exerted equally on both pH and pCO_2 on diel timescales, causing separation of their diel or tidal relationships during

certain seasons. Despite known temporal variability on shorter timescales, discrete sampling was generally representative of the average carbonate system and average air-sea CO_2 flux on a seasonal and annual basis when compared with sensor data.

1. Introduction

Coastal waters, especially estuaries, experience substantial spatial and temporal heterogeneity in water chemistry—including carbonate chemistry parameters such as pH and partial pressure of CO_2 (pCO_2)—due to the diversity of co-occurring biogeochemical and anthropogenic processes (Hofmann et al., 2011; Waldbusser and Salisbury, 2014). Carbonate chemistry is important because an addition of CO_2 acidifies seawater, and acidification can negatively affect marine organisms (Barton et al., 2015; Bednaršek et al., 2012; Ekstrom et al., 2015; Gazeau et al., 2007; Gobler and Talmage, 2014). Additionally, despite the small surface area of coastal waters relative to the global ocean, coastal waters are recognized as important contributors in global carbon cycling (Borges, 2005; Cai, 2011; Laruelle et al., 2018).

While carbonate chemistry, acidification, and air-sea CO_2 fluxes are relatively well studied and understood in open ocean environments, large uncertainties remain in coastal environments. Estuaries are especially challenging to fully understand because of the heterogeneity between and within estuaries that is driven by diverse processes operating on different time scales such as river discharge, nutrient and organic matter loading, stratification, and coastal upwelling (Jiang et al., 2013; Mathis et al., 2012). The traditional sampling method for carbonate system characterization involving discrete water sample collection and laboratory analysis is known to lead to biases in average pCO_2 and CO_2 flux calculations due to daytime sampling that neglects to capture diel

variability (Li et al., 2018). Mean diel ranges in pH can exceed 0.1 unit in many coastal environments, and especially high diel ranges (even exceeding 1 pH unit) have been reported in biologically productive areas or areas with higher mean pCO_2 (Challener et al., 2016; Cyronak et al., 2018; Schulz and Riebesell, 2013; Semesi et al., 2009; Yates et al., 2007). These diel ranges can far surpass the magnitude of the changes in open ocean surface waters that have occurred since the start of the industrial revolution and rival spatial variability in productive systems, indicating their importance for a full understanding of the carbonate system.

Despite the need for high-frequency measurements, sensor deployments have been limited in estuarine environments (especially compared to their extensive use in the open ocean) because of the challenges associated with ~~varying conditions~~highly variable salinities, biofouling, and sensor drift (Sastri et al., 2019). Carbonate chemistry monitoring in the Gulf of Mexico (GOM), has been relatively minimal compared to the United States east and west coasts. The GOM estuaries currently have less exposure to concerning levels of acidification than other estuaries because of their high temperatures (causing water to hold less CO_2 and support high productivity year-round) and often suitable river chemistries (i.e., relatively high buffer capacity) (McCutcheon et al., 2019; Yao et al., 2020). However, respiration-induced acidification is present in both the open GOM (e. g., subsurface water influenced by the Mississippi River Plume and outer shelf region near the Flower Garden Banks National Marine Sanctuary) and GOM estuaries, and most estuaries in the northwestern GOM have also experienced long-term acidification (Cai et al., 2011; Hu et al., 2018, 2015; Kealoha et al., 2020; McCutcheon et al., 2019; Robbins and Lisle, 2018). This ~~known acidification~~evidence of acidification as

well as the relatively high CO_2 efflux from the estuaries of the northwest GOM illustrates the necessity to study the baseline variability and driving factors of carbonate chemistry in the region. In this study, we explored temporal variability in the carbonate system in Aransas Ship Channel (ASC)—a tidal inlet where the lagoonal estuaries meet the coastal waters in a semi-arid region of the northwestern GOM—using both discrete bottle sample collection and hourly sensor measurements, and we explored the driving factors of that variability using data from other co-located environmental sensors. The characterization of carbonate chemistry and consideration of regional drivers can provide context to acidification and its impacts and improved estimates of air-sea CO_2 fluxes.

2. Materials and Methods

2.1 Location

Autonomous sensor monitoring and discrete water sample collections for laboratory analysis of carbonate system parameters were performed in ASC (located at 27˚50'17"N, 97˚3'1"W). ASC is one of the few permanent tidal inlets that intersect a string of barrier islands and connect the GOM coastal waters with the lagoonal estuaries in the northwest GOM (Fig. 1). ASC provides the direct connection between the northwestern GOM and the Mission-Aransas Estuary (Copano and Aransas Bays) to the north and Nueces Estuary (Nueces and Corpus Christi Bays) to the south (Fig. 1). The region is microtidal, with a small tidal range relative to many other estuaries, ranging from ~ 0.6 m tides on the open coast to less than 0.3 m in upper estuaries (Montagna et al., 2011). Mission-Aransas Estuary (MAE) is fed by two small rivers, the Mission (1787 km^2 drainage basin) and Aransas (640 km^2 drainage basin) Rivers (http://waterdata.usgs.gov/), which both experience low base flows punctuated by

periodic high flows during storm events. MAE has an average residence time of one year (Solis and Powell, 1999), so there is a substantial lag between time of rainfall and riverine delivery to ASC in the lower estuary. A significant portion of riverine water flowing into Aransas Bay originates from the larger rivers further northeast on the Texas coast via the Intracoastal Waterway (i.e., Guadalupe River (26,625 km^2 drainage basin) feeds San Antonio Bay and has a much shorter residence time of nearly 50 days) (Solis and Powell, 1999; USGS, 2001).

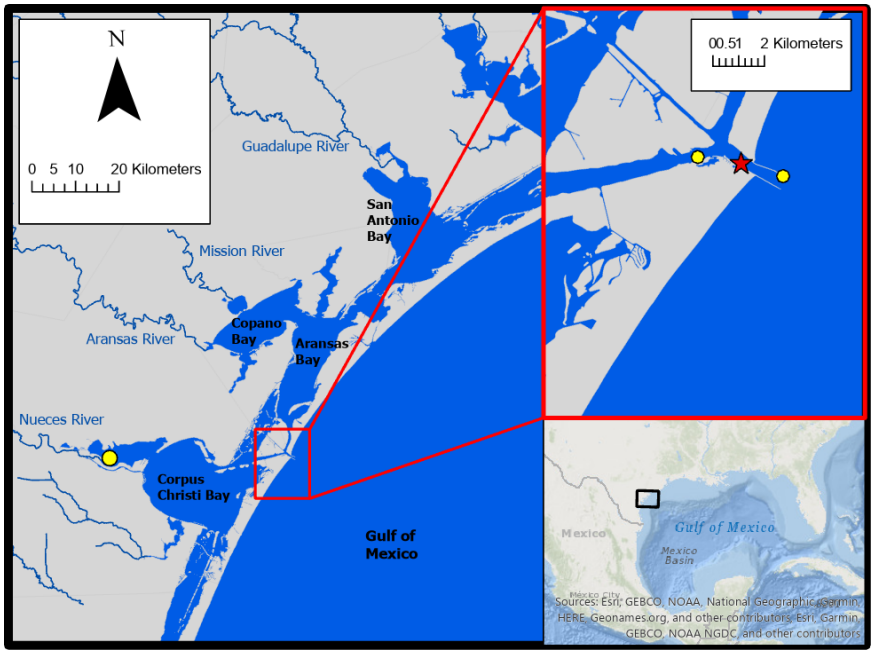

Figure 1. Study area. The location of monitoring in the Aransas Ship Channel (red star) and the locations of NOAA stations used for wind data (yellow circles) are shown.

2.2 Continuous Monitoring

Autonomous sensor monitoring (referred to throughout as continuous monitoring) of pH and pCO_2 was conducted from Nov. 8, 2016 to Aug. 23, 2017 at the University of

Texas Marine Science Institute's research pier in ASC. Hourly pH data were collected using an SAtlantic® SeaFET pH sensor (on total pH scale) and hourly pCO_2 data were collected using a Sunburst® SAMI-CO_2. The pH and pCO_2 sensors were placed in a flowthrough system that received surface water from ASC using a time-controlled diaphragm pump ~~-~~prior to each measurement. Hourly temperature and salinity data were measured by a YSI® 600OMS V2 sonde. All hourly data were single measurements taken on the hour. The average difference between sensor pH and discrete quality assurance samples measured spectrophotometrically in the lab was used to establish a correction factor (-0.05) across the entire sensor pH dataset. Note, this correction scheme was not ideal (Bresnahan et al., 2014) although less rigorous correction based on sensor and discrete pH values has also been used (Shadwick et al. 2019). Nevertheless, the overall good agreement between discrete and corresponding sensor pH values during the deployment period suggested that the SeaFET sensor remained stable. It is also worth noting that our monitoring setup remained free from biofouling during the 10-month period. We attribute this to the deployment design in which the high frequency movement of the pumping mechanisms in the diaphragm pump must have eliminated the influence of animal larvae. ~~The average difference between sensor pH and discrete quality assurance samples measured spectrophotometrically in the lab was used to establish a correction (-0.05) based on a single calibration point across the entire sensor pH dataset (Bresnahan et al., 2014).~~ See supplemental materials for additional sensor deployment and quality assurance information.

2.3 Discrete Sample Collection and Sample Analysis

Long-term monitoring via discrete water sample collection was conducted at ASC from May 2, 2014 to February 25, 2020 (in addition to the discrete, quality assurance sample collections). A single, discrete, surface water sample was collected every two weeks during the summer months and monthly during the winter months from a small vessel at a station near (<20 m from) the sensor deployment. Water sample collection followed standard protocol for ocean carbonate chemistry studies (Dickson et al., 2007). Ground glass borosilicate bottles (250 mL) were filled with surface water and preserved with 100 µL saturated mercury chloride ($HgCl_2$). Apiezon® grease was applied to the bottle stopper, which was then secured to the bottle using a rubber band and a nylon hose clamp.

These samples were used for laboratory dissolved inorganic carbon (DIC) and pH measurements. DIC was measured by injecting 0.5 mL of sample into 1 ml 10% H_3PO_4 (balanced by 0.5 M NaCl) with a high-precision Kloehn syringe pump. The CO_2 gas produced through sample acidification was then stripped using high-purity nitrogen gas and carried into a Li-Cor infrared gas detector. DIC analyses had a precision of 0.1%. Certified Reference Material (CRM) was used to ensure the accuracy of the analysis (Dickson et al. 2003). For samples with salinity>20, pH was measured using a spectrophotometric method at 25 ± 0.1°C (Carter et al. 2003) and the Douglas and Byrne (2017) equation. Analytical precision of the spectrophotometric method for pH measurement was ±0.0004 pH units. A calibrated Orion Ross glass pH electrode was used to measure pH at 25 ± 0.1°C for samples with salinity<20, and analytical precision was ±0.01 pH units. All pH values obtained using the potentiometric method were

converted to total scale at *in situ* temperature (Millero 2001). Salinity of the discrete samples was measured using a benchtop salinometer calibrated by MilliQ water and a known salinity CRM. For discrete samples, pCO_2 was calculated in CO2Sys for Excel using laboratory-measured salinity, DIC, pH, and *in situ* temperature for calculations. Carbonate speciation calculations were done using Millero (2010) carbonic acid dissociation constants (K_1 and K_2), Dickson (1990) bisulfate dissociation constant, and Uppström (1974) borate concentration.

2.4 Calculation of CO_2 fluxes

Equation 1 was used for air-water CO_2 flux calculations (Wanninkhof, 1992; Wanninkhof et al., 2009). Positive flux values indicate CO_2 emission from the water into the atmosphere (the estuary acting as a source of CO_2), and negative flux values indicate CO_2 uptake by the water (the estuary acting as a sink for CO_2).

$$F = k K_0 (pCO_{2,w} - pCO_{2,a}) \quad (1)$$

where k is the gas transfer velocity (in m d^{-1}), K_0 (in mol l^{-1} atm^{-1}) is the solubility constant of CO_2 (Weiss, 1974), and $pCO_{2,w}$ and $pCO_{2,a}$ are the partial pressure of CO_2 (in µatm) in the water and air, respectively.

We used the wind speed parameterization for gas transfer velocity (*k*) from Jiang et al. (2008) converted from cm h^{-1} to m d^{-1}, which is thought to be the best estuarine parameterization at this time (Crosswell et al., 2017), as it is a composite of *k* over several estuaries. The calculation of *k* requires a windspeed at 10 m above the surface, so windspeeds measured at 3 m above the surface were converted using the power law wind profile (Hsu, 1994; Yao and Hu, 2017). To assess uncertainty, other parameterizations with direct applications to estuaries in the literature were also used to calculate CO_2 flux

189 (Raymond and Cole 2001; Ho et al. 2006). We note that parameterization of *k* based on
190 solely windspeed is flawed because several additional parameters can contribute to
191 turbulence including turbidity, bottom-driven turbulence, water-side thermal convection,
192 tidal currents, and fetch (Wanninkhof 1992, Abril et al., 2009, Ho et al., 2104, Andersson
193 et al., 2017), however it is currently the best option for this system given the limited
194 investigations of CO_2 flux and contributing factors in estuaries.

195 Hourly averaged windspeed data for use in CO_2 flux calculations were retrieved
196 from the NOAA-controlled Texas Coastal Ocean Observation Network (TCOON;
197 https://tidesandcurrents.noaa.gov/tcoon.html). Windspeed data from the nearest TCOON
198 station (Port Aransas Station – located directly in ASC, < 2 km inshore from our
199 monitoring location) was prioritized when data were available. During periods of missing
200 windspeed data at the Port Aransas Station, wind speed data from TCOON's Aransas
201 Pass Station (< 2 km offshore from monitoring location) were next used, and for all
202 subsequent gaps, data from TCOON's Nueces Bay Station (~ 40 km away) were used
203 (Fig. 1; additional discussion of flux calculation and windspeed data can be found in
204 supplementary materials). For flux calculations from continuous monitoring data, each
205 hourly measurement of pCO_2 was paired with the corresponding hourly averaged
206 windspeed. For flux calculations from discrete sample data, the pCO_2 calculated for each
207 sampled day was paired with the corresponding daily averaged windspeed (calculated
208 from the retrieved hourly averaged windspeeds).

209 Monthly mean atmospheric xCO_2 data (later converted to pCO_2) for flux
210 calculations were obtained from NOAA's flask sampling network of the Global
211 Monitoring Division of the Earth System Research Laboratory at the Key Biscayne (FL,

212 USA) station. Global averages of atmospheric xCO_2 were used when Key Biscayne data
213 were unavailable. Each pCO_2 observation (whether using continuous or discrete data)
214 was paired with the corresponding monthly averaged xCO_2 for flux calculations.
215 Additional information and justification are available in supplemental materials.

216 *2.5 Additional data retrieval and data processing to investigate carbonate system*
217 *variability and controls*

218 All reported annual mean values are seasonally weighted to account for
219 disproportional sampling between seasons. However, reported annual standard deviation
220 is associated with the un-weighted, arithmetic mean (Table S1). Temporal variability was
221 investigated in the form of seasonal and diel variability (Tables S1, S2, S3). For seasonal
222 analysis, December to February was considered winter, March to May was considered
223 spring, June to August was considered summer, and September to November was
224 considered fall. It is important to note that the Fall season had much fewer continuous
225 sensor observations than other seasons because of the timing of sensor deployment. For
226 diel comparisons, daytime and nighttime variables were defined as 09:00-15:00 local
227 standard time and 21:00-03:00 local standard time, respectively, based on the 6-hour
228 periods with highest and lowest photosynthetically active radiation (PAR; data from co-
229 located sensor, obtained from the Mission-Aransas National Estuarine Research Reserve
230 (MANERR) at https://missionaransas.org/science/download-data). Diel ranges in
231 parameters were calculated (daily maximum minus daily minimum) and only reported for
232 days with the full 24 hours of hourly measurements (176 out of 262 measured days) to
233 ensure that data gaps did not influence the diel ranges (Table S3).

Controls on pCO_2 from thermal and non-thermal (i.e., combination of physical and biological) processes were investigated following Takahashi et al. (2002) over annual, seasonal, and daily time scales using both continuous and discrete data. Over any given time period, this method uses the ratio of the ranges of temperature-normalized pCO_2 ($pCO_{2,nt}$, Eq. 2) and the mean annual pCO_2 perturbed by the difference between mean and observed temperature ($pCO_{2,t}$, Eq. 3) to calculate the relative influence of non-thermal and thermal effects on pCO_2 (T/B, Eq. 4). When calculating annual T/B values with discrete data, only complete years (sampling from January to December) were included (2014 and 2020 were omitted). When calculating daily T/B values with continuous data, only complete days (24 hourly measurements) were included.

$$pCO_{2,nt} = pCO_{2,obs} \times \exp[\delta \times (T_{mean} - T_{obs})] \quad (2)$$

$$pCO_{2,t} = pCO_{2,mean} \times \exp[\delta \times (T_{obs} - T_{mean})] \quad (3)$$

where the value for δ (0.0411 $°C^{-1}$), which represents average [$\partial \ ln \ pCO_2 \ / \ \partial$ Temperature] from field observations, was taken directly from Yao and Hu (2017), T_{obs} is the observed temperature, and T_{mean} is the mean temperature over the investigated time period.

$$T/B = \frac{\max(pCO_{2,thermal}) - \min(pCO_{2,thermal})}{\max(pCO_{2,non-thermal}) - \min(pCO_{2,non-thermal})} \quad (4)$$

Where a T/B greater than one indicates that temperature's control on pCO_2 is greater than the control from non-thermal factors and a T/B less than one indicates that non-thermal factors' control on pCO_2 is greater than the control from temperature.

Tidal control on parameters was investigated using our continuous monitoring data and tide level data obtained from NOAA's Aransas Pass Station (the Aransas Pass

Station used for windspeed data, < 2 km offshore from monitoring location, Fig. 1) at https://tidesandcurrents.noaa.gov/waterlevels.html?id=8775241&name=Aransas,%20Aransas%20Pass&state=TX. Hourly measurements of water level were merged with our sensor data by date and hour. Given that there were gaps in available water level measurements (and no measurements prior to December 20, 2016), the usable dataset was reduced from 6088 observations to 5121 observations and fall was omitted from analyses. To examine differences between parameters during high tide and low tide, we defined high tide as tide level greater than the third quartile tide level value and low tide as a tide level less than the first quartile tide level value.

Other factors that may exert control on the carbonate system were investigated through parameter relationships. In addition to previously discussed tide and windspeed data, we obtained dissolved oxygen (DO), PAR, turbidity, and chlorophyll fluorescence data from MANERR-deployed environmental sensors that were co-located at our monitoring location (obtained from https://missionaransas.org/science/download-data). Given that MANERR data are all measured in the bottom water (>5 m) while our sensors were measuring surface waters, we excluded the observations with significant water column stratification (defined as a salinity difference > 3 between surface water and bottom water) from analyses. Omitting stratified water reduced our continuous dataset from 6088 to 5524 observations (removing 260 winter, 133 spring, 51 summer, and 120 fall observations), and omitting observations where there were no MANERR data to determine stratification further reduced the dataset to 4112 observations. Similarly, removing instances of stratification reduced discrete sample data from 104 to 89 surface water observations.

279 *2.6 Statistical Analyses*

280 All statistical analyses were performed in R, version 4.0.3 (R Core Team, 2020).
281 To investigate differences between daytime and nighttime parameter values (temperature,
282 salinity, pH, pCO_2, and CO_2 flux) using continuous monitoring data across the full
283 sampling period and within each season, paired *t*-tests were used, pairing each respective
284 day's daytime and nighttime values (Table S3). We also used loess models (locally
285 weighted polynomial regression) to identify changes in diel patterns over the course of
286 our monitoring period.

287 Two-way ANOVAs were used to examine differences in parameter means
288 between seasons and between monitoring methods (Table S2). Since there were
289 significant interactions (between season and sampling type factors) in the two-way
290 ANOVAs for each individual parameter (Table S2), differences between seasons were
291 investigated within each monitoring method (one-way ANOVAs) and the differences
292 between monitoring methods were investigated within each season (one-way ANOVAs).
293 For the comparison of monitoring methods, we included both the full discrete sampling
294 data as well as a subset of the discrete sampling data to overlap with the continuous
295 monitoring period (referred to throughout as reduced discrete data or D_C) along with the
296 continuous data. To interpret differences between monitoring methods, a difference in
297 means between the continuous monitoring and discrete monitoring datasets would only
298 indicate that the 10-month period of continuous monitoring was not representative of the
299 5+ year period that discrete samples have been collected, but a difference in means
300 between the continuous data and discrete sample data collected during the continuous
301 monitoring period represents discrepancies between types of monitoring. Post-hoc

multiple comparisons (between seasons within sampling types and between sampling types within seasons) were conducted using the Westfall adjustment (Westfall, 1997).

Differences in parameters between high tide and low tide conditions were investigated using a two-way ANOVA to model parameters based on tide level and season. In models for each parameter, there was a significant interaction between tide level and season factors (based on α=0.05, results not shown), thus t-tests were used (within each season) to examine differences in parameters between high and low tide conditions. Note that fall was omitted from this analysis because tide data were only available at the location beginning December 20, 2016. Sample sizes were the same for each parameter (High tide – winter: 354, spring: 569, summer: 350; Low tide – winter: 543, spring: 318, summer: 415).

Additionally, to gain insight to carbonate system controls through correlations, we conducted Pearson correlation analyses to examine individual correlations of pH and pCO_2 (both continuous and discrete) with other environmental parameters (Table S5).

To better understand overall system variability over different time scales, we used a linear discriminant analysis (LDA), a multivariate statistic that allows dimensional reduction, to determine the linear combination of environmental parameters (individual parameters reduced into linear discriminants, LDs) that allow the best differentiation between day and night as well as between seasons. We included pCO_2, pH, temperature, salinity, tide level, wind speed, total PAR, DO, turbidity, and fluorescent chlorophyll in this analysis. All variables were centered and scaled to allow direct comparison of their contribution to the system variability. The magnitude (absolute value) of coefficients of the LDs (Table 1) represents the relative importance of each individual environmental

parameter in the best discrimination between day and night and between seasons, i.e., the greater the absolute value of the coefficient, the more information the associated parameter can provide about whether the sample came from day or night (or winter, spring, or summer). Only one LD could be created for the diel variability (since there are only two classes to discriminate between – day and night). Two LDs could be created for the seasonal variability (since there were three classes to discriminate between – fall was omitted because of the lack of tidal data), but we chose to only report the coefficients for LD1 given that LD1 captured 95.64% of the seasonal variability.

3. Results

3.1 Seasonal variability

Both the continuous and discrete data showed substantial seasonal variability for all parameters (Fig. 2, Tables S1 and S2). All discrete sample results reported here are for the entire 5+ years of monitoring; the subset of discrete sample data that overlaps with the continuous monitoring period will be addressed only in the discussion for method comparisons (Section 4.1.1). Both continuous and discrete data demonstrate significant differences in temperature between each season, with the highest temperature in summer and the lowest in winter (Tables S1 and S2). Mean salinity during sampling periods was highest in the summer and lowest in the fall (Table S1). Significant differences in seasonal salinity occurred between all seasons except spring and winter for continuous data, but only summer differed from other seasons based on discrete data (Tables S1 and S2).

Carbonate system parameters also varied seasonally (Fig. 2). For both continuous and discrete data, winter had the highest seasonal pH (8.19 ± 0.08 and 8.162 ± 0.065, respectively) and lowest seasonal pCO_2 (365 ± 44 µatm and 331 ± 39 µatm, respectively), while summer had the lowest seasonal pH (8.05 ± 0.06 and 7.975 ± 0.046, respectively) and highest seasonal pCO_2 (463 ± 48 µatm and 511 ± 108, respectively) (Fig. 2, Table S1). All seasonal differences in pH and pCO_2 were significant, except for the discrete data spring versus fall for both parameters (Table S2).

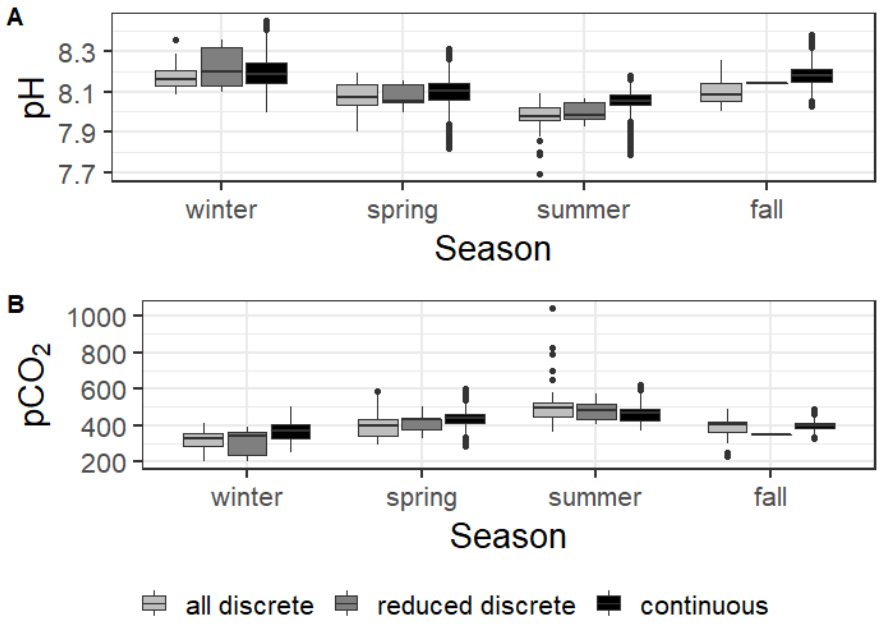

Figure 2. Boxplots of seasonal variability in pH and pCO_2 using all discrete data, reduced discrete data (to overlap with continuous monitoring, Nov. 8 2016 – Aug 23, 2017), and continuous sensor data.

Mean CO_2 flux differed by season (Fig. 3, Tables S1 and S2). Both continuous and discrete data records resulted in net negative CO_2 fluxes during fall and winter months, with winter being most negative. Both methods reported a net positive flux for summer, while spring fluxes were positive according to continuous data and negative according to the 5+ years of discrete data (Fig. 3, Table S1). Annual net CO_2 fluxes were near zero (Table S1).

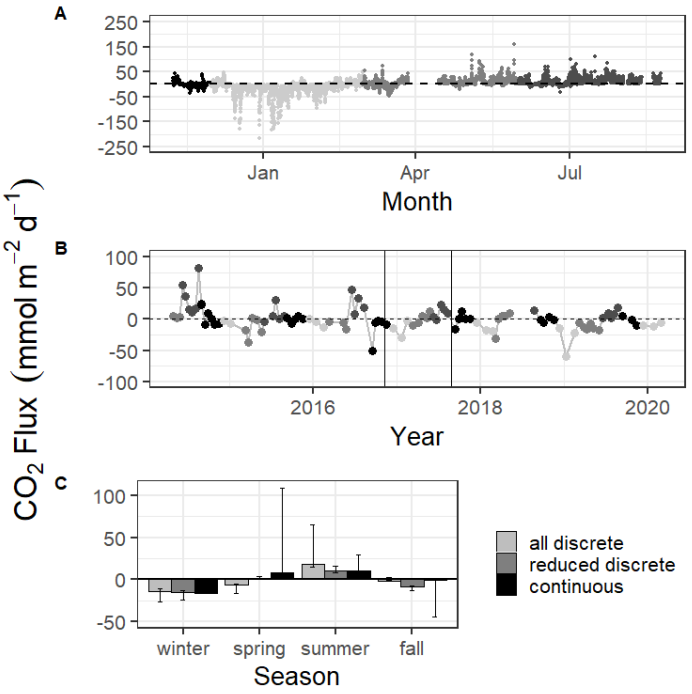

Figure 3. CO_2 flux calculated over the sampling periods from continuous (A) and discrete (B) data. Gray scale in (A) and (B) denote different seasons. Vertical lines in (B) denote the time period of continuous monitoring. (C) shows the seasonal mean CO_2 flux. Error bars represent mean CO_2 flux using Ho (2006) and Raymond and Cole (2001) windspeed parameterizations.

Results of the LDA incorporated carbonate system parameters along with additional environmental parameters to get a full picture of system variability over seasonal timescales (Table 1). The most important parameter in system variability that allowed differentiation between seasons was temperature (Table 1, Seasonal LD1), as would be expected with the clear seasonal temperature fluctuations (Fig. S1E). The second most important parameter for seasonal differentiation was chlorophyll, likely indicating clear seasonal phytoplankton blooms. The carbonate chemistry also played a critical role in seasonal differentiation, as pCO_2 was the third most important factor (Table 1).

Table 1. Coefficients of linear discriminants (LD) from LDA using continuous sensor data and other environmental parameters. Discriminants for both diel and seasonal variability shown.

	Seasonal	**Diel**
	LD1	**LD1**
Temperature (°C)	-3.53	0.54
Salinity	0.04	0.15
pCO_2 (µatm)	-0.29	-0.16
pH	0.10	0.06
Tide Level (m)	-0.24	0.10
Wind speed (ms^{-1})	0.05	-0.00
Total PAR	-0.07	-2.29
DO ($mg\ L^{-1}$)	0.09	-0.08
Turbidity	0.15	-0.06
Fluor. Chlorophyll	-0.40	0.14

3.2 Diel variability

The 10 months of in-situ continuous monitoring revealed that there was substantial diel variability in measured parameters (Fig. 4, Table S3). Temperature had a mean diel range of 1.3 ± 0.8°C (Table S3). Daytime and nighttime temperature differed significantly during the summer and fall months, with higher temperatures at night for both seasons (Table S3). The mean diel range of salinity was 3.4 ± 2.7 (Table S3). Daytime and nighttime salinity differed significantly during the winter and fall months,

with higher salinities at night for both seasons. The mean diel range of pH was 0.09 ± 0.05 (Table S3). Daytime and nighttime pH differed significantly during the winter, summer, and fall, with nighttime pH significantly higher during summer and winter and lower during fall (Fig. 4, Table S3). The mean diel range of pCO_2 was 58 ± 33 µatm (Fig. 4, Table S3). Daytime and nighttime pCO_2 differed significantly during the winter and summer months, with nighttime pCO_2 significantly higher during the summer and lower during the winter (Fig. 4, Table S3). No significant difference in daytime and nighttime DO were observed during any season (Fig. 5F; paired t-tests, winter $p = 0.1573$, spring $p = 0.4877$, summer $p = 0.794$).

Loess models that investigated the evolution of day-night difference in parameters revealed that other environmental parameters, including salinity, temperature, and tide level, also had diel patterns that varied over the duration of our continuous monitoring (Fig. 5).

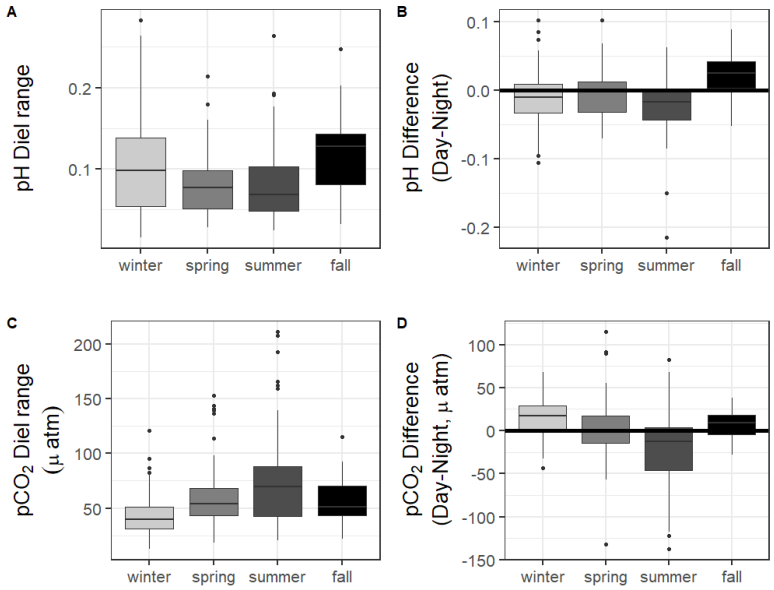

Figure 4. Boxplots of the diel range (maximum minus minimum) and difference in daily parameter mean daytime minus nighttime measurements for pH and pCO_2 from continuous sensor data.

CO_2 flux also fluctuated on a daily scale, with a mean diel range of 34.1 ± 29.0 mmol m^{-2} d^{-1} (Table S3). However, there was not a significant difference in CO_2 flux of daytime versus nighttime hours for the entire monitoring period or any individual season based on α=0.05 (paired t-test, Table S3).

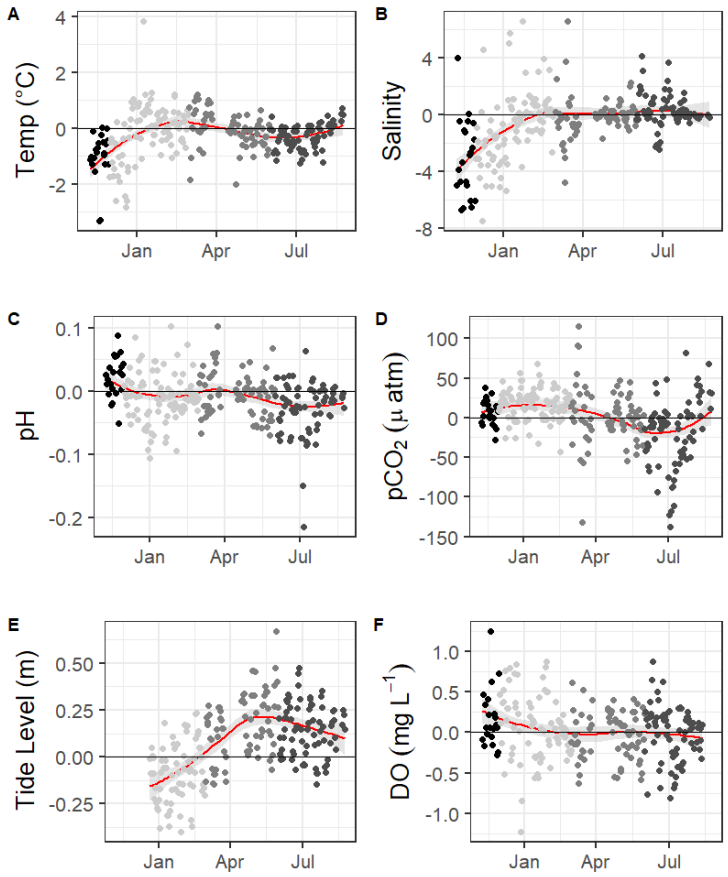

Figure 5. Loess models (red line) and their confidence intervals (gray bands) showing the difference in daily daytime mean minus nighttime mean measurements. The gray scale of the data points represents the four seasons over which data were collected. Data span from Nov 8, 2016 to Aug 3, 2017, except for the tide data, which began December 20, 2016.

Results of the LDA for differentiation between daytime and nighttime conditions revealed that the most important factor was PAR, as would be expected (Table 1, Diel LD1). Temperature was the second most important factor to differentiate between day and night. The carbonate chemistry also played a critical role in day/night differentiation,

as pCO_2 was the third most important parameter, providing more evidence for differentiation between day and night than other parameters that would be expected to vary on a diel timescale (e.g., chlorophyll and DO) (Table 1).

3.3 Controlling factors and correlates

The relative influence of thermal and non-thermal factors (T/B) in controlling pCO_2 varied over different time scales (Fig. 6, Table S4). Based on continuous data, non-thermal processes generally exerted more control than thermal processes (T/B<1) over the entire 5+ years of discrete monitoring, within each season, and over most (167/178) days (Fig. 6, Table S4). Annual T/B from discrete data ranged from 0.50 to 1.16, with only one of the five sampled years having T/B greater than one (i.e., more thermal influence; Table S4). While most individual seasons that were sampled experienced stronger non-thermal control on pCO_2 (T/B <1), the only season that never experienced stronger thermal control was summer, with summer T/B values ranging from 0.21 – 0.35 for the 6 sampled years (Table S4).

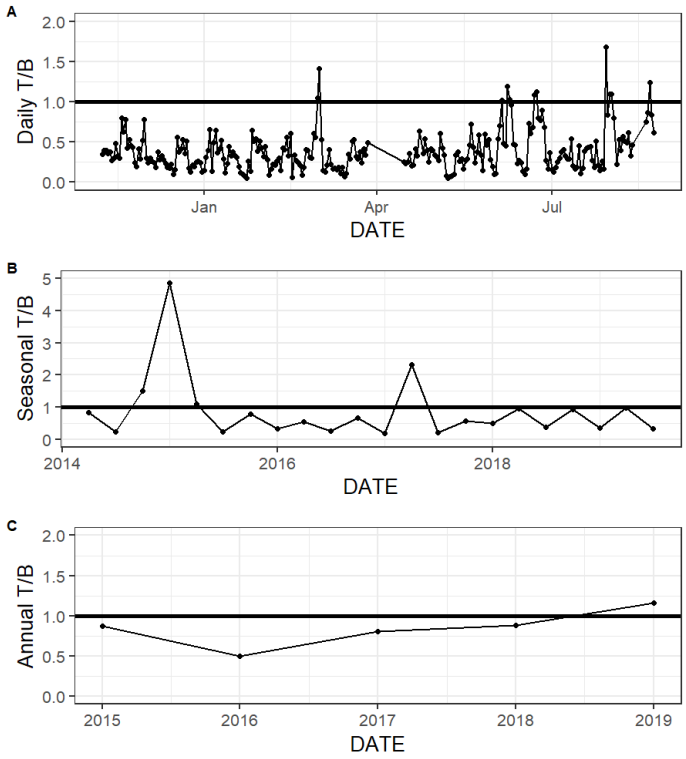

446

447 **Figure 6.** Thermal versus non-thermal control on pCO_2 daily (A), seasonal (B), and
448 annual (C) time scales using both continuous sensor data (daily, from Nov 8, 2016 to Aug
449 3, 2017) and discrete sample data (seasonal and annual, from May 2, 2014- Feb. 25, 2020).
450

451 Tidal fluctuations seemed to have a significant effect on carbonate system
452 parameters (Table 2). Both temperature and salinity were higher at low tide during the
453 winter and summer months and higher at high tide during the spring. pCO_2 was higher
454 during low tide during all seasons. pH was higher during high tide during the winter and
455 summer, but this reversed during the spring, when pH was higher at low tide. CO_2 flux
456 also varied with tidal fluctuations. CO_2 flux was higher (more positive or less negative) in
457 the low tide condition for all seasons (though the difference was not significant in

458 spring), i.e., the location was less of a CO_2 sink during low tide conditions in the winter
459 and more of a CO_2 source during low tide conditions in the summer.

460

461 **Table 2.** Mean and standard deviation of temperature, salinity, pH, pCO_2, and calculated
462 CO_2 flux (from continuous sensor measurements) during high and low tide conditions.
463

Parameter	Season	High Tide Mean	Low Tide Mean	Difference between tide levels, t-test p-value
Temperature (°C)	Winter	16.7 ± 1.7	17.6 ± 2.0	**<0.0001**
	Spring	24.4 ± 2.7	23.6 ± 2.7	**<0.0001**
	Summer	29.3 ± 0.5	30.1 ± 0.7	**<0.0001**
Salinity	Winter	30.2 ± 2.5	31.3 ± 2.9	**<0.0001**
	Spring	30.4 ± 1.9	30.0 ± 2.7	**0.0071**
	Summer	30.5 ± 2.4	34.5 ± 3.0	**<0.0001**
pH	Winter	8.20 ± 0.08	8.15 ± 0.06	**<0.0001**
	Spring	8.07 ± 0.09	8.10 ± 0.07	**<0.0001**
	Summer	8.08 ± 0.04	8.04 ± 0.06	**<0.0001**
pCO_2 (µatm)	Winter	331 ± 40	378 ± 42	**<0.0001**
	Spring	435 ± 33	443 ± 50	**0.0154**
	Summer	419 ± 30	482 ± 48	**<0.0001**
CO_2 Flux ($mmol\ m^{-2}\ d^{-1}$)	Winter	-33.0 ± 38.1	-11.7 ± 21.8	**<0.0001**
	Spring	7.4 ± 14.0	8.7 ± 14.8	**0.2248**
	Summer	1.8 ± 6.3	16.0 ± 14.5	**<0.0001**

464

465 Mean water level varied between all seasons; mean spring (highest) water levels
466 were on average 0.08 m higher than winter (lowest) water levels (ANOVA $p<0.0001$, fall
467 was not considered because of a lack of water level data). The mean daily tidal range
468 during our continuous monitoring period was 0.39 m ± 0.13 m, which did not
469 significantly differ between seasons (ANOVA $p=0.739$). However, the day-night
470 difference in tide level exhibited a strong seasonality, with spring and summer having
471 higher tide level during the daytime and winter having higher tide level during the
472 nighttime (Fig. 5).

473 There were significant correlations between carbonate system parameters (pH and
474 pCO_2) and many of the other environmental parameters, including windspeed, DO,

turbidity, and fluorescent chlorophyll (Figure 7, Table S5). Both the continuous and discrete sampling types indicate that pH has a significant negative relationship with both temperature and salinity and pCO_2 has a significant positive relationship with both temperature and salinity (Fig. 7). However, correlations with temperature were stronger for continuous data and correlations with salinity were stronger for discrete data (Table S5). The strongest correlations between continuous carbonate system data and all investigated environmental parameters were with DO (positive correlation with pH and negative correlation with pCO_2; Table S5). It is worth noting that there were no observations of hypoxia at our study site during our monitoring, with minimum DO levels of 3.9 mg L^{-1} and 4.0 mg L^{-1} for our continuous monitoring period and our discrete sampling period, respectively.

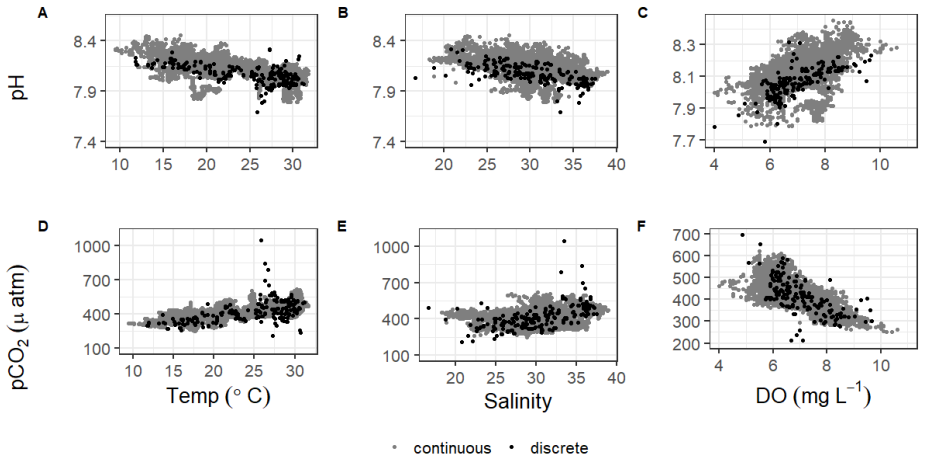

Figure 7. Correlations of pH and pCO_2 with temperature, salinity, and DO from continuous sensor data (gray) and all discrete data (black).

Discussion

4.1 Comparing continuous monitoring and discrete sampling: Representative sampling in a temporally variable environment

Discrete water sample collection and analysis is the most common method that has been employed to attempt to understand the carbonate system of estuaries. However, it is difficult to know if these samples are representative of the spatial and temporal variability in carbonate system parameters. While this time-series study cannot conclude whether our broader sampling efforts in the MAE are representative of the spatial variability in the estuary, it can investigate how representative our bimonthly to monthly sampling is of the more high-frequency temporal variability that ASC experiences.

There were several instances where seasonal parameter means significantly differed between the 10-month continuous monitoring period and the 5+ year discrete sampling period (Table S2, $C \neq D$ or $D_c \neq D$) including temperature in the summer and fall, salinity in the spring, pH in the summer and fall, and pCO_2 in winter, spring, and summer. While clear seasonal variability was demonstrated for most parameters (using both continuous and discrete data for the entire period), these differences between the 10-month continuous monitoring period and our 5+ year monitoring period illustrate that there is also interannual variability in the system. Therefore, short periods of monitoring are unable to fully capture current baseline conditions.

During the continuous monitoring period (2016-2017), we found no significant difference between sampling methods in the seasonal mean temperature, salinity, or pCO_2. The two sampling methods also resulted in the same mean pH for all seasons except for summer, when the sensor data recorded a higher mean pH than discrete

samples (Tables S1 and S2). During this case, we can conclude that discrete monitoring did not accurately represent the system variability that was able to be captured by the sensor monitoring. However, given that most seasons did not show differences in pH or pCO_2 between sampling methods, the descriptive statistics associated with the discrete monitoring did a fair job of representing system means. This is evidence that long-term discrete monitoring efforts, which are much more widespread in estuarine systems than sensor deployments, can be generally representative of the system despite known temporal variability on shorter time scales. However, further study would be needed to determine if this applies throughout the system, as the upper estuary generally experiences greater variability.

Understanding the relationships of pH and pCO_2 with temperature and salinity is important in a system (Fig. 7). Based on the results of an Analysis of Covariance (ANCOVA), the relationship (slope) of pH with both temperature and salinity and of pCO_2 with salinity were not significantly different between types of monitoring (considering the sensor deployment period only), supporting the effectiveness of long-term discrete monitoring programs when sensors are unable to be deployed. However, ANCOVA did reveal the relationship of pCO_2 with temperature is significantly different (method:temp p=0.0062) between monitoring methods.

The high temporal resolution of sensor data is presumably better for estimating CO_2 flux at a given location than discrete sampling. Previous studies have pointed out that discrete sampling methods, which generally involve only daytime sampling, do not adequately capture the diel variability in the carbonate system and may therefore lead to biased CO_2 fluxes (Crosswell et al., 2017; Liu et al., 2016). However, we found no

significant difference (within any season) between CO_2 flux values calculated with hourly sensor data versus single, discrete samples collected monthly to twice monthly (Table S2, Fig. 3). Calculated CO_2 fluxes also did not significantly differ between day and night during any season, despite some differences in pCO_2 (Table S3), likely due to the large error associated with the calculation of CO_2 flux (Table S1, Fig. 3) which will be further discussed below. Therefore, the expected underestimation of CO_2 flux based on diel variability of pCO_2 was not encountered at our study site, validating the use of discrete samples for quantification of CO_2 fluxes (until methods with less associated error are available). Even given less error in calculated flux, estimated fluxes would likely not differ between methods on an annual scale (as pCO_2 did not), but CO_2 fluxes may differ on a seasonal scale since the differences between daytime and nighttime pCO_2 were not consistent across seasons (Table S3, Fig. 4).

There are many factors contributing to error associated with CO_2 flux. There is still large error associated with estimates of estuarine CO_2 flux because turbulent mixing is difficult to model and turbulence is the main control on CO_2 gas transfer velocity, k, in shallow water environments. Thus, our wind speed parameterization of k is imperfect and likely the greatest source of error (Borges and Abril, 2011; Van Dam et al., 2019). Other notable sources of error include the data treatment. For example, we chose to seasonally weight the individual calculated flux values in the calculation of annual flux to account for differences in sampling frequency between seasons. From continuous data, the weighted average flux was 0.2 mmol m^{-2} d^{-1}, although choosing not to seasonally weight and simply look at the arithmetic mean of fluxes calculated directly from sampling dates would have resulted in an annual CO_2 flux of -0.7 mmol m^{-2} d^{-1} for the same period.

Similarly, the weighted average flux from all 5+ years of discrete data was -0.9 mmol m^{-2} d^{-1}, but the arithmetic mean of fluxes would have resulted in an annual CO_2 flux of 0.2 mmol m^{-2} d^{-1} for the same period. Another source of error that could be associated with the calculation of flux from the discrete data is the way in which wind speed data are aggregated to be used in the windspeed parameterization. We decided to use daily averages of the windspeed for calculations. Using the windspeed measured for the closest time to our sampling time or the monthly averaged wind speed may have resulted in very different flux values.

4.2 Factors controlling temporal variability in carbonate system parameters

Our study site had a relatively small range of pH and pCO_2 on both diel and seasonal scales compared to other coastal regions (Challener et al., 2016; Yates et al., 2007). This small variability is likely tied to a combination of the subtropical setting (small temperature variability), the lower estuary position of our monitoring (further removed from the already small freshwater influence), little ocean upwelling influence, and the system's relatively high buffer capacity that results from the high alkalinity of the freshwater endmembers (Yao et al., 2020). Just as the extent of hypoxia-induced acidification was relatively low in Corpus Christi Bay because of the bay's high buffer capacity (McCutcheon et al., 2019), the extent of pH fluctuation resulting from all controlling factors at ASC would also be modulated by the region's high intrinsic buffer capacity.

4.2.1 Thermal and biological controls on carbonate chemistry

We demonstrated that both temperature and non-thermal processes exert control on pCO_2, but non-thermal control generally surpasses thermal control in ASC over

585 multiple time scales (Fig. 6, Table S4, T/B<1). The magnitude of pCO_2 variation
586 attributed to non-thermal processes varied greatly (i.e., $\Delta pCO_{2,nt}$ had large standard
587 deviations, Table S4). For example, during the year of strongest non-thermal control
588 (2016), $\Delta pCO_{2,nt}$ was 534 µatm versus $\Delta pCO_{2,nt}$ of 209 µatm in the year of weakest
589 thermal control (2019). Conversely, the magnitude of pCO_2 variation attributed to
590 temperature was consistent across time scales. For example, during the year of strongest
591 thermal control (2015), $\Delta pCO_{2,t}$ was 276 µatm versus $\Delta pCO_{2,t}$ of 242 µatm in the year of
592 weakest thermal control (2017). Spring and fall seasons, which experienced the greatest
593 temperature swings (Table S1), had greater relative temperature control exerted on pCO_2
594 out of all seasons (Fig. 6, Table S4). The difference in T/B between sampling methods is
595 relatively small over the 10-month sensor deployment period, but it is worth noting that
596 T/B did not align over shorter seasonal time scales sampling methods (Fig. 6, Table S4).
597 Continuous monitoring demonstrated a greater magnitude of fluctuation resulting from
598 both temperature and non-thermal processes (i.e., greater $\Delta pCO_{2,t}$ and $\Delta pCO_{2,nt}$),
599 indicating that the extremes are generally not captured by the discrete, daytime sampling,
600 and sensor data would provide a better understanding of system controls.
601 The greater influence of non-thermal controls that we report conflicts with Yao
602 and Hu (2017), who found that ASC was primarily thermally controlled (T/B 1.53 – 1.79)
603 from May 2014 to April 2015. Yao and Hu (2017) also found that locations in the upper
604 estuary experienced lower T/B during flooding conditions than drought conditions.
605 Although the opposite was found at ASC, it is likely that the high T/B calculated at ASC
606 by Yao and Hu (2017) was still a result of the drought condition due to the long residence
607 time of the estuary. Since 2015, there has not been another significant drought in the

608 system, so it seems that non-thermal controls on pCO_2 are more important at this location
609 under normal freshwater inflow conditions.
610 Significantly warmer water temperatures were observed during the nighttime in
611 both summer and fall (Fig. 5), indicating that temperature could exert a slight control on
612 the carbonate system over a diel time scale. We note that significant differences in day
613 and night temperature within seasons do not indicate that diel differences were observed
614 on all days within the season, as large standard deviations in both daytime and nighttime
615 values result in considerable overlap. More substantial temperature swings between
616 seasons would result in more temperature control over a seasonal timescale. ASC seems
617 to have less thermal control of the carbonate system than offshore GOM waters, as
618 temperature had substantially higher explanatory value for pH and pCO_2 based on simple
619 linear regressions in offshore GOM waters (R^2 = 0.81 and 0.78, respectively (Hu et al.,
620 2018)) than at ASC (R^2 = 0.30 and 0.52, respectively, for sensor data and R^2 = 0.38 and
621 0.25, respectively, for discrete data).
622 Though annual average pCO_2 (and CO_2 flux) are higher in the upper MAE and
623 lower offshore than at our study site, the same seasonal patterns that we observed (i.e.,
624 elevated pCO_2 and positive CO_2 flux in the summer and depressed pCO_2 and negative
625 CO_2 flux during the winter, Table S1, Fig. S1) has also been observed throughout the
626 entire MAE and the open Gulf of Mexico (Hu et al., 2018; Yao and Hu, 2017). These
627 seasonal patterns correspond with both the directional response of the system to
628 temperature and net community metabolism response to changing temperature, i.e.,
629 elevated respiration in summer months (Caffrey, 2004). Despite that there were no
630 observations of hypoxia, there was a strong relationship between the carbonate system

parameters and DO (Fig. 7, Table S5), suggesting that net ecosystem metabolism may exert an important control on the carbonate system on seasonal time scales. The lack of day-night difference in DO (Fig. 5F) despite the significant day-night difference in both pH and pCO_2 suggests that net community metabolism is likely not a strong controlling factor on diel time scales. Biological control likely becomes more important over seasonal timescales.

4.2.2 Tidal control on carbonate chemistry

While the tidal range in the northwestern GOM is relatively small (1.30 m over our 10-month continuous monitoring period), the tidal inlet location of our study site results in proportionally more "coastal water" during high tide and proportionally more "estuarine water" during low tide. The carbonate chemistry signal of these different water masses was seen in the differences between high tide and low tide conditions at ASC (i.e., high tide having lower pCO_2 because coastal waters are less heterotrophic than estuarine waters, Table 2). Consequently, the relative importance of thermal versus non-thermal controls may be modulated by tide level. We calculated the thermal and non-thermal pCO_2 terms separately during high tide and low tide periods and found that non-thermal control is more important during low tide conditions (within each season T/B is 0.10 ± 0.07 lower during the low tide than high tide). This is likely because low tide has proportionally more "estuarine water" at the location and because there is less volume of water for the end products of biological processes to accumulate. The difference in T/B between high tide and low tide conditions was greatest in the spring, likely due to a combination of elevated spring-time productivity and larger tidal ranges in the spring.

653 The GOM is one of the few places in the world that experiences diurnal tides
654 (Seim et al., 1987; Thurman, 1994), so theoretically, the fluctuations in pCO_2 associated
655 with tides may align to either amplify or reduce/reverse the fluctuations that would result
656 from diel variability in net community metabolism. Based on diel tidal fluctuations at this
657 site (i.e., higher tides during the day in the spring and summer and higher tides at night
658 during the winter, Fig. 5E) and the higher pCO_2 associated with low tide (Table 2), tidal
659 control should amplify the biological signal (nighttime pCO_2 > daytime pCO_2) during
660 spring and summer and reduce or reverse the biological signal during the winter. This
661 tidal control can explain the diel variability present in our pCO_2 data, which showed the
662 full reversal of the expected biological signal in the winter (Fig. 5C, Table S3, nighttime
663 pCO_2 < daytime pCO_2), i.e., the higher nighttime tides in winter brought in enough low
664 CO_2 water from offshore to fully offset any nighttime buildup of CO_2 from the lack of
665 photosynthesis. However, we note that the expected diel, biological control was likely
666 minimal since daytime DO was not consistently higher than nighttime DO (Fig. 5F). The
667 same seasonal pattern diel tide fluctuations were exhibited from Dec 20, 2016 (when the
668 tide data is first available) through the rest of our discrete monitoring period (Feb 25,
669 2020), indicating that tidal control on diel variability of carbonate system parameters was
670 likely consistent throughout this 3+ year period. The diel variability in pH did not mirror
671 pCO_2 as would be expected (Fig. 5). The relationship between pH and tide level more
672 closely mirrored the relationships of salinity and temperature with tide level (versus pCO_2
673 relationship with tide level; Table 2), indicating that controlling factors of the carbonate
674 system may not be exerted equally on both pH and pCO_2 over different time scales.
675 *4.2.3 Salinity and freshwater inflow controls on carbonate chemistry*

Previous studies have indicated that freshwater inflow may exert a primary control on the carbonate system in the estuaries of the northwestern GOM (Hu et al., 2015; Yao et al., 2020; Yao and Hu, 2017). Though the river water still has elevated pCO_2 and depressed pH compared to the seawater endmember, the high riverine alkalinity (often higher than the seawater endmember) in the region results in relatively well-buffered estuarine conditions in MAE (Yao and Hu, 2017). Carbonate system variability is much lower at ASC than it is in the more upper reaches of MAE, likely due to the lesser influence of freshwater inflow and its associated changes in biological activity at ASC (Yao and Hu, 2017). Given the location of our sampling in the lower portion of the estuary and the long residence time in the system, we did not directly address river discharge as a controlling factor, but the influence of freshwater inflow may be evident in the response of the system to changes in salinity. Fluctuating salinity at ASC may also result from direct precipitation, stratification, and tidal fluctuations; however, the low R^2 (0.02) associated with a simple linear regression between tide level and salinity ($p<0.0001$) indicates that salinity fluctuations are more indicative of non-tidal factors. Salinity data from both sensor and discrete monitoring were strongly correlated with both pH and pCO_2, with correlation coefficients nearing (continuous) or surpassing (discrete) that of the correlations with temperature (Fig. 7; Table S5). Periods of lower salinity had higher pH and lower pCO_2, likely due to enhanced freshwater influence and subsequent elevated primary productivity at the study site.

4.2.4 Windspeed and CO_2 inventory

We investigated wind speed as a possible control on the carbonate system to gain insight into the effect of wind-driven CO_2 fluxes on the inventory of CO_2 in the water

699 column (and subsequent impacts to the entire carbonate system). The Texas coast has
700 relatively high wind speeds, with the mean wind speed observed during our continuous
701 monitoring period being 5.8 m s^{-1}. While this results in relatively high calculated CO_2
702 fluxes (Fig. 3), the seasonal relationship between pCO_2 and windspeed does not support a
703 change in inventory with higher winds. Since spring and summer both have a mean
704 estuarine pCO_2 greater than atmospheric level (and positive CO_2 flux, Table S1) a
705 negative relationship between windspeed and pCO_2 would be necessary to support this
706 hypothesis, but winter, spring, and fall all experience increases in pCO_2 with increasing
707 wind based on simple linear regression.

708 *4.3 Carbonate chemistry as a component of overall system variability*

709 Estuaries and coastal areas are dynamic systems with human influence, riverine
710 influence, and influence from an array of biogeochemical processes, resulting in highly
711 variable environmental conditions. Based on an LDA used to assess overall system
712 variability using a suite of environmental parameters compiled at a single location, we
713 can conclude that carbonate chemistry parameters are among the most important of
714 variants on both daily and seasonal time scales in this coastal setting. Of the two
715 carbonate system components that we incorporated (pH and pCO_2), pCO_2 was the most
716 critical in discriminating along diel or seasonal scales despite similar seasonal differences
717 that were identified by ANOVA (Table S2) and more seasons with significant diel
718 differences in pH (Table S3). pH seemed to be a larger component of overall system
719 variability on a seasonal time scale (compared to the very small contribution seen on a
720 diel scale, Table 1). Given that the seasonal and diel variability in carbonate chemistry at
721 this location is relatively small compared to other coastal areas that are in the literature,

722 the high contribution of carbonate chemistry to overall system variability that we detected
723 is likely to be present at other coastal locations around the world.

724 **5. Conclusions**

725 We monitored carbonate chemistry parameters (pH and pCO_2) using both sensor
726 deployments (10 months) and discrete sample collection (5+ years) at the Aransas Ship
727 Channel, TX, to characterize temporal variability. Significant seasonal variability and
728 diel variability in carbonate system parameters were both present at the location. Diel
729 fluctuations were smaller than many other areas previously studied. The difference
730 between daytime and nighttime values of carbonate system parameters varied between
731 seasons, occasionally reversing the expected diel variability due to biological processes.
732 Tide level (despite the small tidal range), temperature, freshwater influence, and
733 biological activity all seem to exert important controls on the carbonate system at the
734 location. The relative importance of the different controls varied with timescale, and
735 controls were not always exerted equally on both pH and pCO_2. Carbonate chemistry
736 (particularly pCO_2) was among the most important environmental parameters to in
737 overall system variability to distinguish between both diel and seasonal environmental
738 conditions.

739 Despite known temporal variability on shorter timescales, discrete sampling was
740 generally representative of the average carbonate system on a seasonal and annual basis
741 based on comparison with our sensor data. Discrete data captured interannual variability,
742 which could not be captured by the shorter-term continuous sensor data. Additionally,
743 there was no difference in CO_2 flux between sampling types. All of these findings

support the validity of discrete sample collection for carbonate system characterization at this location.

This is one of the first studies that investigates high-temporal frequency data from deployed sensors that measure carbonate system parameters in an estuary-influenced environment. Long-term, effective deployments of these monitoring tools could greatly improve our understanding of estuarine systems. This study's detailed investigation of data from multiple, co-located environmental sensors was able to provide insight into potential driving forces of carbonate chemistry on diel and seasonal time scales; this provides strong support for the implementation of carbonate chemistry monitoring in conjunction with preexisting coastal environmental monitoring infrastructure. Strategically locating such sensors in areas that are subject to local acidification drivers or support large biodiversity or commercially important species may be the most crucial in guiding future mitigation and adaptation strategies for natural systems and aquaculture facilities.

Data availability

Continuous sensor data are archived with the National Oceanic and Atmospheric Administration's (NOAA's) National Centers for Environmental Information (NCEI) (https://doi.org/10.25921/dkg3-1989). Discrete sample data are available in two separate datasets archived with National Science Foundation's Biological & Chemical Oceanography Data Management Office (BCO-DMO) (doi:10.1575/1912/bco-dmo.784673.1 and doi: 10.26008/1912/bco-dmo.835227.1).

Author Contribution

MM and XH defined the scope of this work. XH received funding for all components of the work. MM, HY, and CJS performed field sampling and laboratory analysis of samples. MM prepared the initial manuscript and all co-authors contributed to revisions.

Competing interests

The authors declare that they have no conflict of interest.

Acknowledgements

Funding for autonomous sensors and sensor deployment was provided by the United States Environmental Protection Agency's National Estuary Program via the Coastal Bend Bays and Estuaries Program Contract No. 1605. Thanks to Rae Mooney from Coastal Bend Bays and Estuaries Program for assistance in the initial sensor setup. Funding for discrete sampling as well MM's dissertation research has been supported by both NOAA National Center for Coastal Ocean Science (Contract No. NA15NOS4780185) and NSF Chemical Oceanography Program (OCE-1654232). We also appreciate the support from the Mission-Aransas National Estuarine Research Reserve in allowing us the boat-of-opportunity for our ongoing discrete sample collections and the University of Texas Marine Science Institute for allowing us access to their research pier for the sensor deployment. A special thanks to Hongjie Wang, Lisette Alcocer, Allen Dees, and Karen Alvarado for assistance with field work. We would also like to thank Melissa Ward, our other anonymous referee, and the Associate Editor, Tyler Cyronak, for aiding in the considerable improvement of this manuscript.

References

Barton, A., Waldbusser, G.G., Feely, R.A., Weisberg, S.B., Newton, J.A., Hales, B., Cudd, S., Eudeline, B., Langdon, C.J., Jefferds, I., King, T., Suhrbier, A., Mclaughlin, K., 2015. Impacts of coastal acidification on the pacific northwest shellfish industry and adaptation strategies implemented in response. Oceanography 28, 146–159.

Bednaršek, N., Tarling, G.A., Bakker, D.C.E., Fielding, S., Jones, E.M., Venables, H.J., Ward, P., Kuzirian, A., Lézé, B., Feely, R.A., Murphy, E.J., 2012. Extensive dissolution of live pteropods in the Southern Ocean. Nat. Geosci. 5, 881–885. https://doi.org/10.1038/ngeo1635

Borges, A. V., 2005. Do we have enough pieces of the jigsaw to integrate CO_2 fluxes in the coastal ocean ? Estuaries 28, 3–27.

Borges, A. V., Abril, G., 2011. Carbon Dioxide and Methane Dynamics in Estuaries, Treatise on Estuarine and Coastal Science. https://doi.org/10.1016/B978-0-12-374711-2.00504-0

Bresnahan, P.J., Martz, T.R., Takeshita, Y., Johnson, K.S., LaShomb, M., 2014. Best practices for autonomous measurement of seawater pH with the Honeywell Durafet. Methods Oceanogr. 9, 44–60. https://doi.org/10.1016/j.mio.2014.08.003

Caffrey, J.M., 2004. Factors controlling net ecosystem metabolism in U.S. estuaries. Estuaries 27, 90–101. https://doi.org/10.1007/BF02803563

Cai, W.-J., 2011. Estuarine and Coastal Ocean Carbon Paradox: CO_2 Sinks or Sites of Terrestrial Carbon Incineration? Ann. Rev. Mar. Sci. 3, 123–145. https://doi.org/10.1146/annurev-marine-120709-142723

811 Cai, W.-J., Hu, X., Huang, W.-J., Murrell, M.C., Lehrter, J.C., Lohrenz, S.E., Chou, W.-
812 C., Zhai, W., Hollibaugh, J.T., Wang, Y., Zhao, P., Guo, X., Gundersen, K., Dai, M.,
813 Gong, G.-C., 2011. Acidification of subsurface coastal waters enhanced by
814 eutrophication. Nat. Geosci. 4, 766–770. https://doi.org/10.1038/ngeo1297
815 Challener, R.C., Robbins, L.L., Mcclintock, J.B., 2016. Variability of the carbonate
816 chemistry in a shallow, seagrass-dominated ecosystem: Implications for ocean
817 acidification experiments. Mar. Freshw. Res. 67, 163–172.
818 https://doi.org/10.1071/MF14219
819 Crosswell, J.R., Anderson, I.C., Stanhope, J.W., Van Dam, B., Brush, M.J., Ensign, S.,
820 Piehler, M.F., McKee, B., Bost, M., Paerl, H.W., 2017. Carbon budget of a shallow,
821 lagoonal estuary: Transformations and source-sink dynamics along the river-estuary-
822 ocean continuum. Limnol. Oceanogr. 62, S29–S45.
823 https://doi.org/10.1002/lno.10631
824 Cyronak, T., Andersson, A.J., D'Angelo, S., Bresnahan, P., Davidson, C., Griffin, A.,
825 Kindeberg, T., Pennise, J., Takeshita, Y., White, M., 2018. Short-term spatial and
826 temporal carbonate chemistry variability in two contrasting seagrass meadows:
827 Implications for pH buffering capacities. Estuaries and Coasts 41, 1282–1296.
828 https://doi.org/10.1007/s12237-017-0356-5
829 Dickson, A.G., 1990. Standard potential of the reaction: AgCl(s) + 1 $2H_2$(g) = Ag(s) +
830 HCl(aq), and and the standard acidity constant of the ion HSO4- in synthetic sea
831 water from 273.15 to 318.15 K. J. Chem. Thermodyn. 22, 113–127.
832 https://doi.org/10.1016/0021-9614(90)90074-Z
833 Ekstrom, J. a., Suatoni, L., Cooley, S.R., Pendleton, L.H., Waldbusser, G.G., Cinner, J.E.,

834 Ritter, J., Langdon, C., van Hooidonk, R., Gledhill, D., Wellman, K., Beck, M.W.,
835 Brander, L.M., Rittschof, D., Doherty, C., Edwards, P.E.T., Portela, R., 2015.
836 Vulnerability and adaptation of US shellfisheries to ocean acidification. Nat. Clim.
837 Chang. 5, 207–214. https://doi.org/10.1038/nclimate2508
838 Gazeau, F., Quiblier, C., Jansen, J.M., Gattuso, J.-P., Middelburg, J.J., Heip, C.H.R.,
839 2007. Impact of elevated CO_2 on shellfish calcification. Geophys. Res. Lett. 34,
840 L07603. https://doi.org/10.1029/2006GL028554
841 Gobler, C.J., Talmage, S.C., 2014. Physiological response and resilience of early life-
842 stage Eastern oysters (*Crassostrea virginica*) to past, present and future ocean
843 acidification. Conserv. Physiol. 2, 1–15.
844 https://doi.org/10.1093/conphys/cou004.Introduction
845 Ho, D.T., Law, C.S., Smith, M.J., Schlosser, P., Harvey, M., Hill, P., 2006.
846 Measurements of air-sea gas exchange at high wind speeds in the Southern Ocean:
847 Implications for global parameterizations. Geophys. Res. Lett. 33, 1–6.
848 https://doi.org/10.1029/2006GL026817
849 Hofmann, G.E., Smith, J.E., Johnson, K.S., Send, U., Levin, L. a, Micheli, F., Paytan, A.,
850 Price, N.N., Peterson, B., Takeshita, Y., Matson, P.G., Crook, E.D., Kroeker, K.J.,
851 Gambi, M.C., Rivest, E.B., Frieder, C. a, Yu, P.C., Martz, T.R., 2011. High-
852 frequency dynamics of ocean pH: a multi-ecosystem comparison. PLoS One 6,
853 e28983. https://doi.org/10.1371/journal.pone.0028983
854 Hsu S. A., 1994. Determining the power-law wind-profile exponent under near-neatral
855 stability condidtions at sea. J. Appl. Meteorol. 33, 757–765.
856 Hu, X., Beseres Pollack, J., McCutcheon, M.R., Montagna, P. a., Ouyang, Z., 2015.

857 Long-term alkalinity decrease and acidification of estuaries in Northwestern Gulf of
858 Mexico. Environ. Sci. Technol. 49, 3401–3409. https://doi.org/10.1021/es505945p
859 Hu, X., Nuttall, M.F., Wang, H., Yao, H., Staryk, C.J., McCutcheon, M.R., Eckert, R.J.,
860 Embesi, J.A., Johnston, M.A., Hickerson, E.L., Schmahl, G.P., Manzello, D.,
861 Enochs, I.C., DiMarco, S., Barbero, L., 2018. Seasonal variability of carbonate
862 chemistry and decadal changes in waters of a marine sanctuary in the Northwestern
863 Gulf of Mexico. Mar. Chem. 205, 16–28.
864 https://doi.org/10.1016/j.marchem.2018.07.006
865 Jiang, L.-Q., Cai, W.-J., Wang, Y., 2008. A comparative study of carbon dioxide
866 degassing in river- and marine-dominated estuaries. Limnol. Oceanogr. 53, 2603–
867 2615. https://doi.org/10.4319/lo.2008.53.6.2603
868 Jiang, L.Q., Cai, W.J., Wang, Y., Bauer, J.E., 2013. Influence of terrestrial inputs on
869 continental shelf carbon dioxide. Biogeosciences 10, 839–849.
870 https://doi.org/10.5194/bg-10-839-2013
871 Kealoha, A.K., Shamberger, K.E.F., DiMarco, S.F., Thyng, K.M., Hetland, R.D.,
872 Manzello, D.P., Slowey, N.C., Enochs, I.C., 2020. Surface water CO_2 variability in
873 the Gulf of Mexico (1996–2017). Sci. Rep. 10, 1–13.
874 https://doi.org/10.1038/s41598-020-68924-0
875 Laruelle, G.G., Cai, W.-J., Hu, X., Gruber, N., Mackenzie, F.T., Regnier, P., 2018.
876 Continental shelves as a variable but increasing global sink for atmospheric carbon
877 dioxide. Nat. Commun. 9, 454. https://doi.org/10.1038/s41467-017-02738-z
878 Li, D., Chen, J., Ni, X., Wang, K., Zeng, D., Wang, B., Jin, H., Huang, D., Cai, W.J.,
879 2018. Effects of biological production and vertical mixing on sea surface pCO_2

variations in the Changjiang River Plume during early autumn: A buoy-based time series study. J. Geophys. Res. Ocean. 123, 6156–6173. https://doi.org/10.1029/2017JC013740

Liu, H., Zhang, Q., Katul, G.G., Cole, J.J., Chapin, F.S., MacIntyre, S., 2016. Large CO_2 effluxes at night and during synoptic weather events significantly contribute to CO_2 emissions from a reservoir. Environ. Res. Lett. 11, 1–8. https://doi.org/10.1088/1748-9326/11/6/064001

Mathis, J.T., Pickart, R.S., Byrne, R.H., Mcneil, C.L., Moore, G.W.K., Juranek, L.W., Liu, X., Ma, J., Easley, R.A., Elliot, M.M., Cross, J.N., Reisdorph, S.C., Bahr, F., Morison, J., Lichendorf, T., Feely, R.A., 2012. Storm-induced upwelling of high pCO_2 waters onto the continental shelf of the western Arctic Ocean and implications for carbonate mineral saturation states. Geophys. Res. Lett. 39, 4–9. https://doi.org/10.1029/2012GL051574

McCutcheon, M.R., Staryk, C.J., Hu, X., 2019. Characteristics of the carbonate system in a semiarid estuary that experiences summertime hypoxia. Estuaries and Coasts 42, 1509–1523. https://doi.org/10.1007/s12237-019-00588-0

Millero, F.J., 2010. Carbonate constant for estuarine waters. Mar. Freshw. Res. 61, 139–142.

Montagna, P.A., Brenner, J., Gibeaut, J., Morehead, S., 2011. Chapter 4: Coastal Impacts, in: Jurgen Schmandt, Gerald R. North, and J.C. (Ed.), The Impact of Global Warming on Texas. University of Texas Press, pp. 96–123.

Raymond, P.A., Cole, J.J., 2001. Gas exchange in rivers and estuaries: Choosing a gas transfer velocity. Estuaries 24, 312–317. https://doi.org/10.2307/1352954

Robbins, L.L., Lisle, J.T., 2018. Regional acidification trends in florida shellfish estuaries: a 20+ year look at pH, oxygen, temperature, and salinity. Estuaries and Coasts 41, 1268–1281. https://doi.org/10.1007/s12237-017-0353-8

Sastri, A.R., Christian, J.R., Achterberg, E.P., Atamanchuk, D., Buck, J.J.H., Bresnahan, P., Duke, P.J., Evans, W., Gonski, S.F., Johnson, B., Juniper, S.K., Mihaly, S., Miller, L.A., Morley, M., Murphy, D., Nakaoka, S.I., Ono, T., Parker, G., Simpson, K., Tsunoda, T., 2019. Perspectives on in situ sensors for ocean acidification research. Front. Mar. Sci. 6, 1–6. https://doi.org/10.3389/fmars.2019.00653

Schulz, K.G., Riebesell, U., 2013. Diurnal changes in seawater carbonate chemistry speciation at increasing atmospheric carbon dioxide. Mar. Biol. 160, 1889–1899. https://doi.org/10.1007/s00227-012-1965-y

Seim, H.E., Kjerfve, B., Sneed, J.E., 1987. Tides of Mississippi Sound and the adjacent continental shelf. Estuar. Coast. Shelf Sci. 25, 143–156. https://doi.org/10.1016/0272-7714(87)90118-1

Semesi, I.S., Beer, S., Björk, M., 2009. Seagrass photosynthesis controls rates of calcification and photosynthesis of calcareous macroalgae in a tropical seagrass meadow. Mar. Ecol. Prog. Ser. 382, 41–47. https://doi.org/10.3354/meps07973

Shadwick E. H., Friedrichs M. A. M., Najjar R.G., De Meo, O. A., Friedman, J. R., Da, F. Reay, W. G., 2019. High-Frequency CO_2 System Variability Over the Winter-to-Spring Transition in a Coastal Plain Estuary. J Geophys. Res. Ocean. 124(11): 7626-7642. doi:10.1029/2019JC015246

Solis, R.S., Powell, G.L., 1999. Hydrography, Mixing Characteristics, and Residence Time of Gulf of Mexico Estuaries, in: Bianchi, T.S., Pennock, J.R., Twilley, R.R.

Formatted: Normal (Web), Indent: Left: 0", Hanging: 0.4", Widow/Orphan control, Adjust space between Latin and Asian text, Adjust space between Asian text and numbers

Formatted: Subscript

Formatted: Font: Not Italic

Formatted: Font: Not Italic

Formatted: Font: Not Italic

Formatted: Check spelling and grammar

(Eds.), Biogeochemistry of Gulf of Mexico Estuaries. John Wiley & Sons, Inc: New York, pp. 29–61.

Takahashi, T., Sutherland, S.C., Sweeney, C., Poisson, A., Metzl, N., Tilbrook, B., Bates, N., Wanninkhof, R., Feely, R.A., Sabine, C., Olafsson, J., Nojiri, Y., 2002. Global sea-air CO_2 flux based on climatological surface ocean pCO_2, and seasonal biological and temperature effects. Deep. Res. Part II Top. Stud. Oceanogr. 49, 1601–1622. https://doi.org/10.1016/S0967-0645(02)00003-6

Thurman, H. V., 1994. Introductory Oceanography, Seventh Edition. pp. 252–276.

Uppström, L.R., 1974. The boron/chlorinity ratio of deep-sea water from the Pacific Ocean. Deep. Res. Oceanogr. Abstr. 21, 161–162. https://doi.org/10.1016/0011-7471(74)90074-6

USGS, 2001. Discharge Between San Antonio Bay and Aransas Bay, Southern Gulf Coast, Texas, May-September 1999.

Van Dam, B.R., Edson, J.B., Tobias, C., 2019. Parameterizing Air-Water Gas Exchange in the Shallow, Microtidal New River Estuary. J. Geophys. Res. Biogeosciences 124, 2351–2363. https://doi.org/10.1029/2018JG004908

Waldbusser, G.G., Salisbury, J.E., 2014. Ocean acidification in the coastal zone from an organism's perspective: multiple system parameters, frequency domains, and habitats. Ann. Rev. Mar. Sci. 6, 221–47. https://doi.org/10.1146/annurev-marine-121211-172238

Wanninkhof, R., 1992. Relationship between wind speed and gas exchange. J. Geophys. Res. 97, 7373–7382. https://doi.org/10.1029/92JC00188

Wanninkhof, R., Asher, W.E., Ho, D.T., Sweeney, C., McGillis, W.R., 2009. Advances

949 in quantifying air-sea gas exchange and environmental forcing. Ann. Rev. Mar. Sci.
950 1, 213–244. https://doi.org/10.1146/annurev.marine.010908.163742
951 Weiss, R.F., 1974. Carbon dioxide in water and seawater: the solubility of a non-ideal
952 gas. Mar. Chem. 2, 203–215.
953 Westfall, P.H., 1997. Multiple testing of general contrasts using logical constraints and
954 correlations. J. Am. Stat. Assoc. 92, 299–306.
955 https://doi.org/10.1080/01621459.1997.10473627
956 Yao, H., Hu, X., 2017. Responses of carbonate system and CO_2 flux to extended drought
957 and intense flooding in a semiarid subtropical estuary. Limnol. Oceanogr. 62, S112–
958 S130. https://doi.org/10.1002/lno.10646
959 Yao, H., McCutcheon, M.R., Staryk, C.J., Hu, X., 2020. Hydrologic controls on CO_2
960 chemistry and flux in subtropical lagoonal estuaries of the northwestern Gulf of
961 Mexico. Limnol. Oceanogr. 65, 1380–1398. https://doi.org/10.1002/lno.11394
962 Yates, K.K., Dufore, C., Smiley, N., Jackson, C., Halley, R.B., 2007. Diurnal variation of
963 oxygen and carbonate system parameters in Tampa Bay and Florida Bay. Mar.
964 Chem. 104, 110–124. https://doi.org/10.1016/j.marchem.2006.12.008
965